Electronic Supplementary Material (ESI) for Materials Chemistry Frontiers.

Supporting Information for

Design of Planar-Zigzag Semiconducting Polymers to Control Chain Orientation and Electronic Structure for Organic Photovoltaics

Fengkun Chen,[a] Kyohei Nakano,[a] Yumiko Kaji,[a] Keisuke Tajima*[a]

[a] RIKEN Center for Emergent Matter Science (CEMS), 2-1 Hirosawa, Wako, Saitama 351-0198, Japan

*E-mail: keisuke.tajima@riken.jp

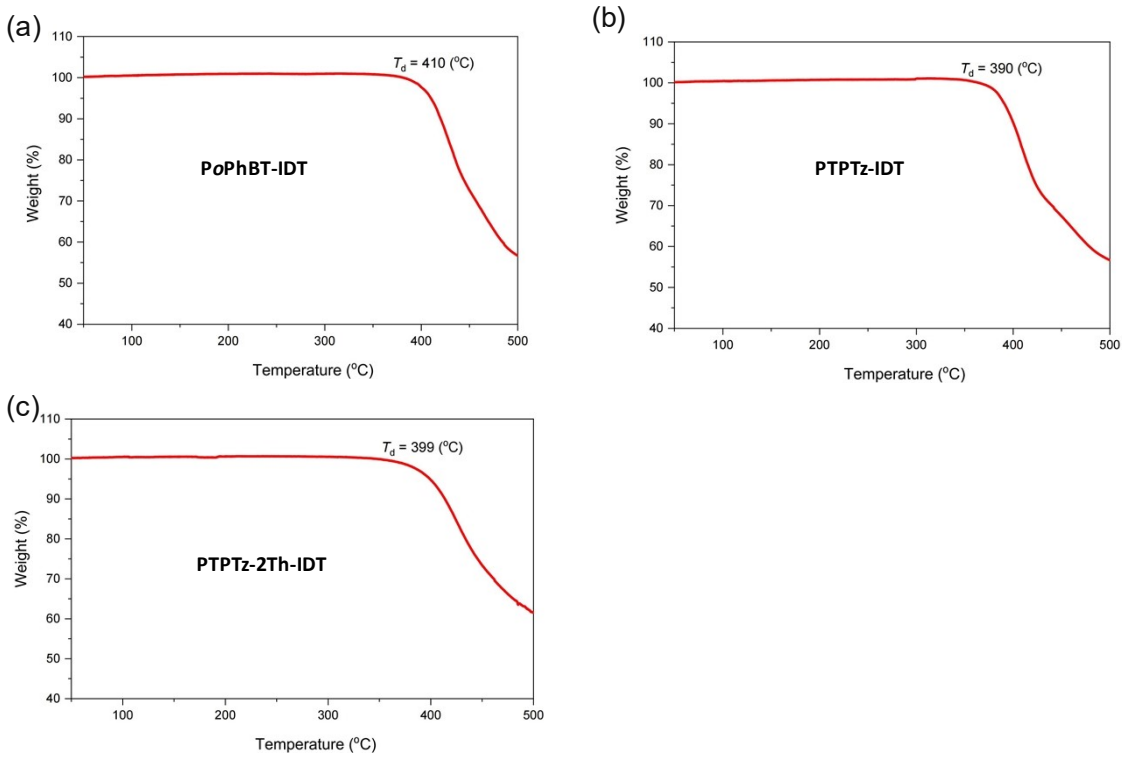

Figure S1. Thermal gravimetric analysis for (a) P*o*PhBT-IDT, (b) PTPTz-IDT, and (c) PTPTz-2Th-IDT. The scan rate is 10 °C/min.

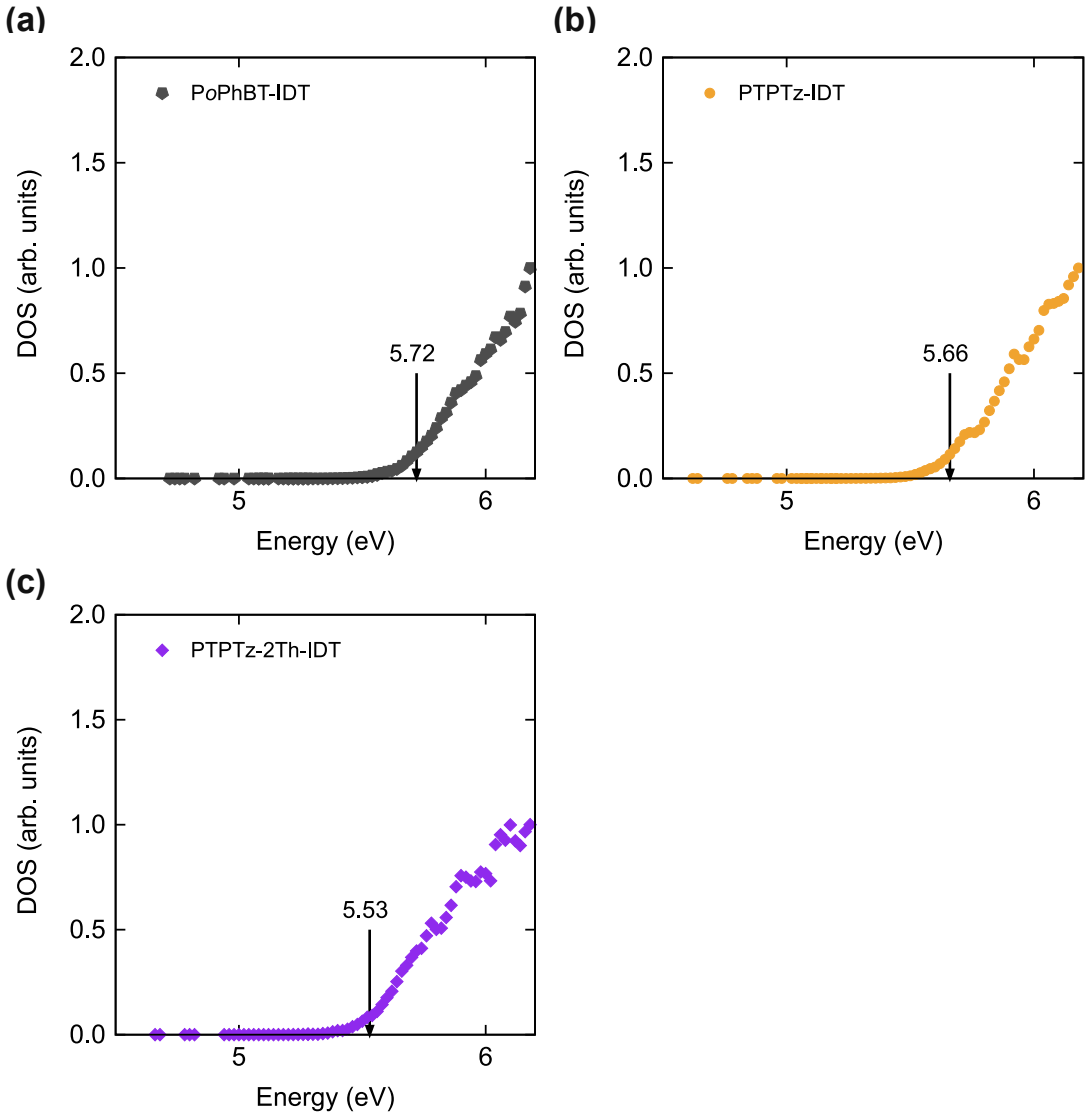

Figure S2. Occupied density of states (DOS) of (a) P*o*PhBT-IDT, (b) PTPTz-IDT, and (c) PTPTz-2Th-IDT determined by photoelectron yield spectroscopy. The DOS edge was fitted using a Gaussian function, and the energy of the highest occupied molecular orbital (E_{HOMO}) was calculated as $E_{HOMO} = E_{PT} - 2\sigma$, where E_{PT} and σ are the peak-top energy and width of the Gaussian function, respectively. The arrows indicate the evaluated E_{HOMO}s.

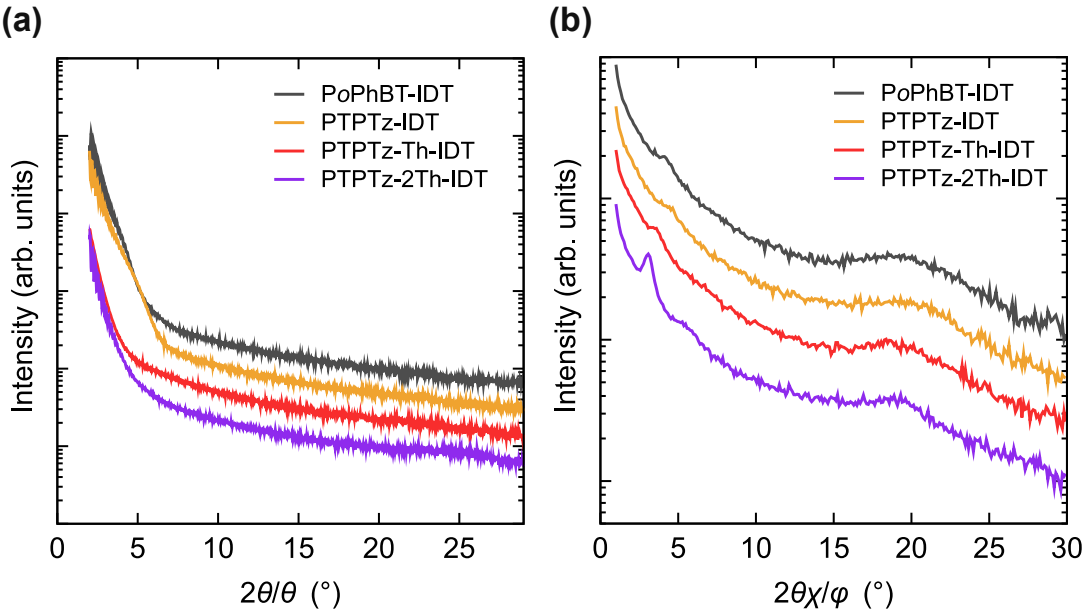

Figure S3. One-dimensional XRD patterns of the pristine polymer films in the (a) out-of-plane and (b) in-plane directions.

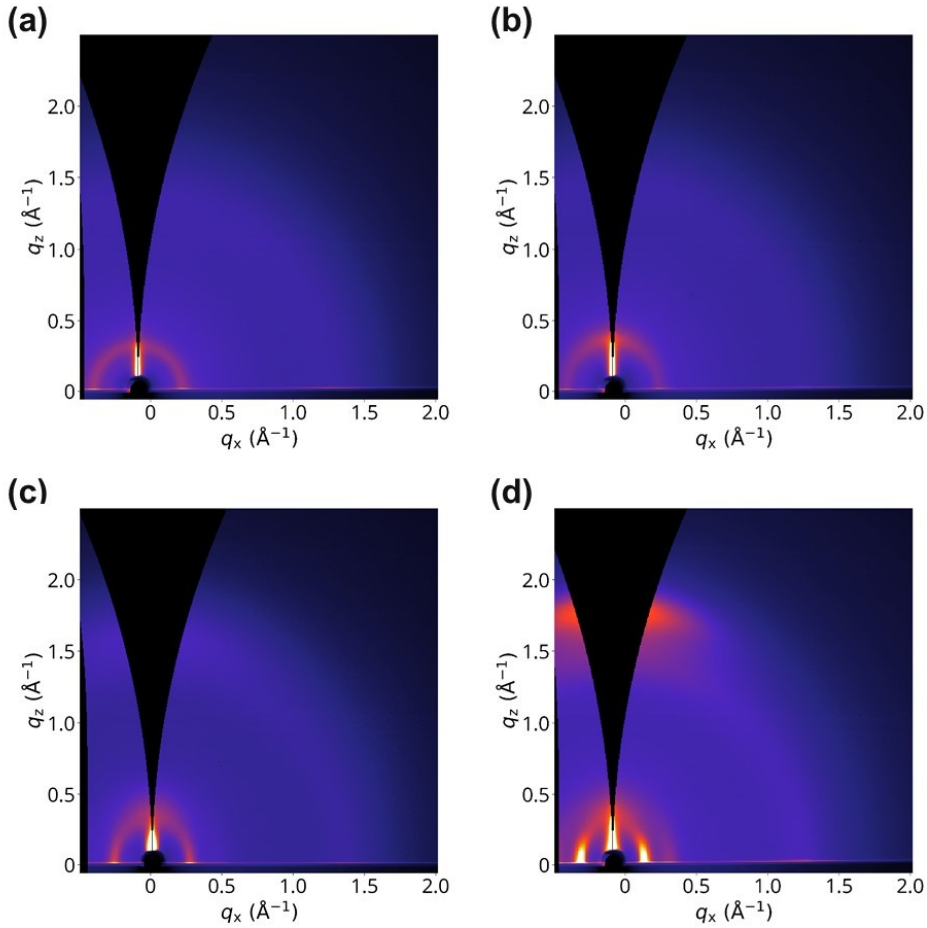

Figure S4. Two-dimensional GIWAXS patterns of the pristine polymer films for (a) P*o*PhBT-IDT, (b) PTPTz-IDT, (c) PTPTz-Th-IDT (ref. S1), and (d) PTPTz-2Th-IDT.

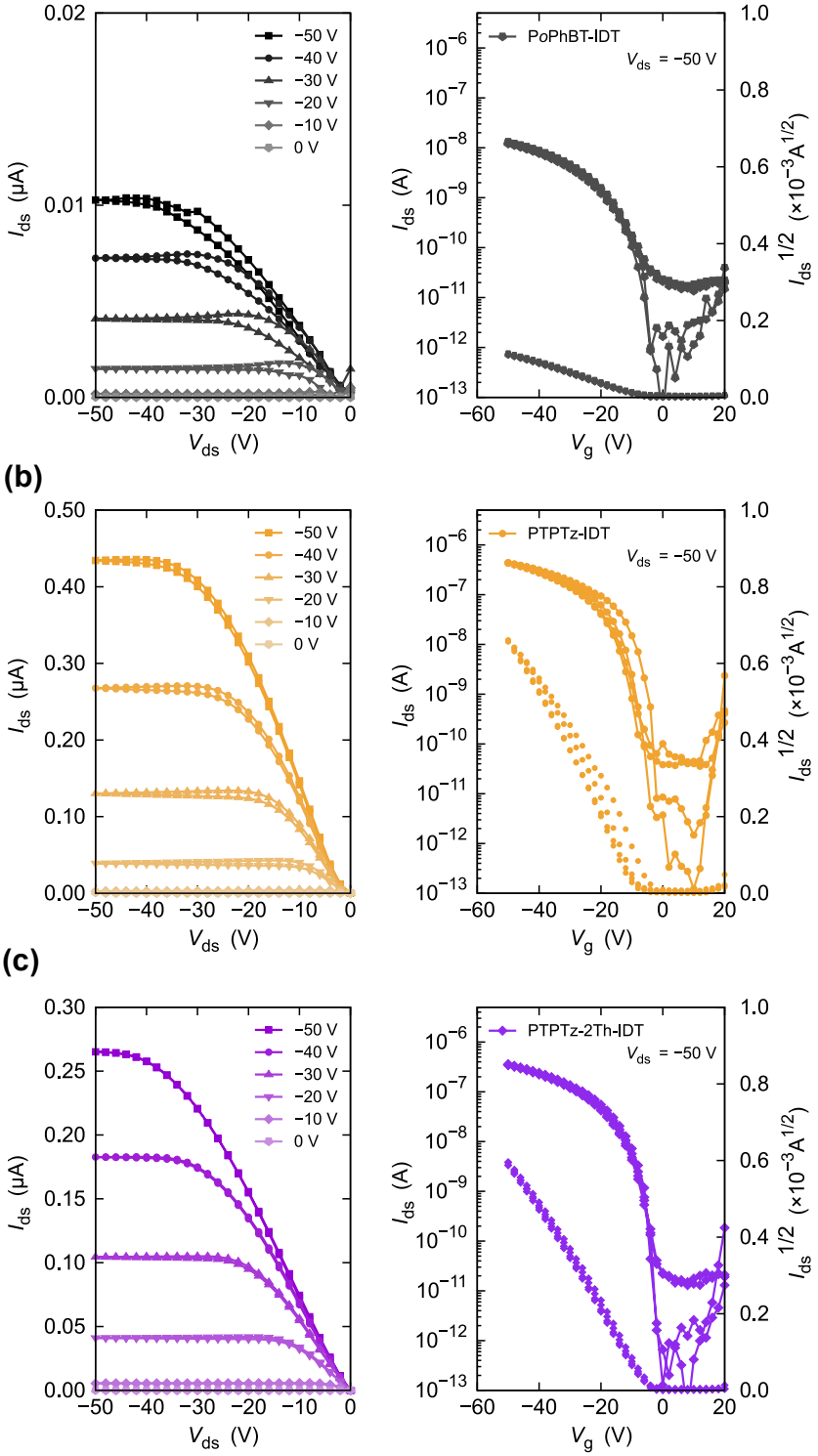

Figure S5. Output and transfer curves of field-effect transistor (FET) devices using (a) P*o*PhBT-IDT, (b) PTPTz-IDT, and (c) PTPTz-2Th-IDT. The saturated FET mobilities were 1.7×10^{-4}, 6.4×10^{-3}, and 5.0×10^{-3} cm^2 V^{-1} s^{-1}, respectively.

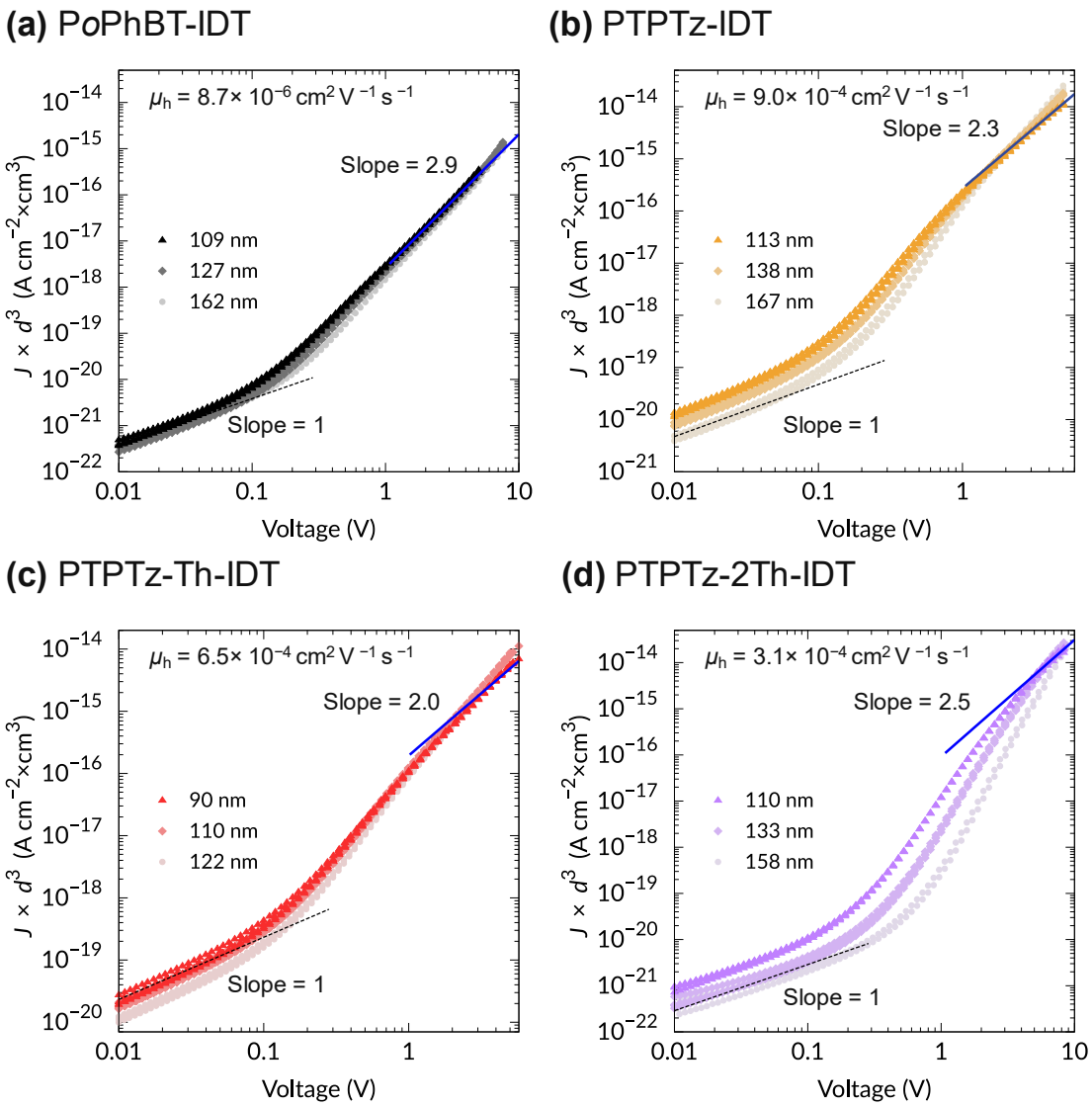

Figure S6. Current density normalized by the cube of the film thickness (*d*) plotted against voltage for the hole-only devices (ITO/PEDOT:PSS/polymer/MoO_3/Ag) with the pristine films. (a) P*o*PhBT-IDT, (b) PTPTz-IDT, (c) PTPTz-Th-IDT (data adopted from ref. S1), and (d) PTPTz-2Th-IDT. The holes were injected from the MoO_3/Ag electrode. The hole mobility was evaluated based on Mott–Gurney law with a permittivity of 3. We assumed that in the high applied voltage regime, where the normalized *J*-*V* curves with different film thicknesses were identical with a slope close to 2, the current flow through the polymer is governed by space charge.

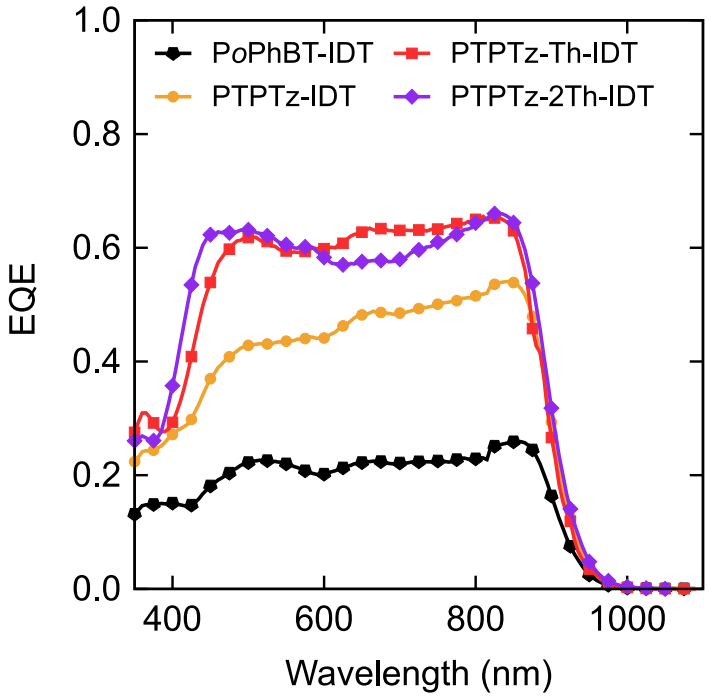

Figure S7. External quantum efficiency (EQE) spectra of the corresponding OSCs.

Table S1. Optimization condition of BHJ devices. The shaded rows show the optimum conditions used in the main text. The acceptor is Y6 for all devices. DIO: 1,8-diiodooctane.

Polymer	D:A	DIO (%)	Annealing (°C/min)	J_{SC} (mA/cm^2)	V_{OC} (V)	FF	PCE (%)
P*o*PhBT-IDT	1:1.3	-	150/10	4.7	0.79	0.41	1.5
	1:1.3	0.5	-	3.7	0.5	0.42	0.79
	1:1.3	0.5	80/10	5.2	0.64	0.43	1.4
	1:1.3	0.5	120/10	6.2	0.73	0.43	2.0
	1:1.3	0.5	150/10	7.7	0.75	0.42	2.4
	1:1.3	0.5	180/10	6.6	0.78	0.43	2.2
PTPTz-IDT	1:2.0	0.5	150/10	13.1	0.84	0.61	6.7
	1:1.3	-	150/10	11.8	0.85	0.57	5.8
	1:1.3	0.25	150/10	12.8	0.84	0.60	6.5
	1:1.3	0.5	150/10	15.4	0.84	0.61	7.9
	1:1.3	0.5	-	10.5	0.64	0.49	3.3
	1:1.3	1.0	150/10	16.0	0.83	0.62	8.2
	1:1.3	1.0	180/10	15.5	0.83	0.62	8.0
	1:1.3	1.0	200/10	15.1	0.84	0.61	7.7
	1:1.3	1.0	250/10	2.6	0.79	0.43	0.9
	1:1.3	1.25	150/10	15.9	0.82	0.61	7.9
	1:1.3	1.5	150/10	15.5	0.82	0.61	7.7
	1:1.3	1.75	150/10	15.1	0.81	0.60	7.2
	1:1.3	2.0	150/10	14.8	0.81	0.59	7.1
	1:0.75	0.5	150/10	12.8	0.86	0.60	6.7
	1:0.5	0.5	150/10	11.2	0.86	0.57	5.5
PTPTz-2Th-IDT	1:2	0.5	150/10	17.6	0.77	0.58	7.8
	1:1.3	-	150/10	17.4	0.78	0.46	6.3
	1:1.3	0.25	150/10	19.0	0.77	0.54	7.8
	1:1.3	0.5	-	17.5	0.68	0.43	5.1
	1:1.3	0.5	120/10	19.7	0.75	0.57	8.4
	1:1.3	0.5	150/10	19.5	0.75	0.58	8.5
	1:1.3	0.5	180/10	20.0	0.75	0.60	9.0
	1:1.3	0.5	200/10	20.3	0.75	0.58	8.7
	1:1.3	0.5	250/10	2.0	0.70	0.43	0.6
	1:1.3	1.0	150/10	19.8	0.72	0.55	7.8
	1:0.75	0.5	150/10	14.9	0.76	0.45	5.1
	1:0.5	0.5	150/10	3.0	0.67	0.19	0.4

Instrumentation

Silica gel column chromatography was performed on Wakogel C-300 (FUJIFILM Wako Pure Chemical Corporation). Thin-layer chromatography was carried out on aluminum sheets coated with silica gel 60 F254 (Merck 5554, Merck Millipore). ^{1}H and ^{13}C NMR spectra were recorded on an NMR spectrometer (JNM-ECZ400, JEOL) operating at 400 MHz for ^{1}H NMR and 100 MHz for ^{13}C NMR, and using the residual solvent as the internal reference for ^{1}H (δ = 7.26 ppm in $CDCl_3$) and for ^{13}C (δ = 77.16 ppm in $CDCl_3$) spectra at room temperature. High-resolution mass spectrometry (HRMS) was performed on a mass spectrometer (JMS-T100GCV, JEOL).

Polymerization was conducted with a microwave reactor (Initiator+, Biotage). Gel permeation chromatography was performed on a high-performance liquid chromatography system (Prominence, Shimadzu) equipped with a UV detector and size exclusion columns at 40 °C using chloroform and calibrated with polystyrene standards.

Thermogravimetric analysis was performed on a differential thermogravimetric analyzer (TG 8120, Rigaku) at a heating rate of 10 °C min^{-1} under N_2 with runs recorded from room temperature to 500 °C. Differential scanning calorimetry was performed on a calorimeter (DSC 8230, Rigaku) with a heating/cooling rate of 10 °C/min under N_2 flow. Al_2O_3 was used as a reference compound.

Substrate preparation: All substrates were cleaned by sequential ultrasonication in detergent solution, water, 2-propanol, and acetone, followed by O_2 plasma treatment.

Photoelectron yield spectroscopy measurements: Photoelectron yield spectroscopy was performed with photoemission yield spectroscopy in air systems (AC-2 and AC-3, RIKEN KEIKI) with a monochromated D2 lamp. The films were prepared on a glass substrate coated with conductive indium tin oxide (ITO). The occupied density of states was obtained by calculating the central differential of the yield with energy, as reported previously.[S2]

Field-effect transistor device fabrication and characterization: The surface of pre-cleaned n+Si substrates with a 300 nm SiO_2 insulating layer (E&M) was covered with an octadecyltrimethoxysilane self-assembled monolayer (SAM). The SAM formation conditions were the same as reported (with trichloroethylene).[S3] Polymer films approximately 50 nm thick were spin-coated onto the other glass substrate and transferred to the SAM by the contact film transfer method.[S4] A 15-nm-thick Au and 25-nm-thick Ag top-contact electrode were formed sequentially by thermal evaporation through a

metal shadow mask under a pressure of 10^{-4} Pa. The channel width and length were 1000 and 200 μm, respectively. Source meters were used to measure the source-drain current (6430, Keithley) and gate leakage current (2400, Keithley). Field-effect transistor measurements were conducted in a vacuum of ~10^{-2} Pa.

Organic photovoltaic device fabrication: A pre-cleaned glass substrate with a patterned ITO electrode was used. The ITO surface was covered by an approximately 30-nm-thick ZnO nanoparticle layer, as previously reported.[S5] A donor polymer:Y6 (4.0:5.3 mg mL^{-1}) chloroform solution with optimized concentration of 1,8-diiodooctane was spin-coated on the ZnO layer at 500 rpm, resulting in a film about 100 nm thick. The film was thermally annealed at the optimized temperature prior to the back-electrode evaporation. A MoO_3 hole-transporting layer (10 nm) and Ag electrodes (100 nm) were deposited by thermal evaporation through a metal mask under a high vacuum (~10^{-4} Pa). The device area was 0.165 cm^2. We encapsulated all samples with a glass cap and UV-curable resin in a dry N_2-filled glovebox.

Current-voltage characteristics: The current-voltage characteristics of the devices were measured under simulated solar illumination (AM1.5, 100 mW cm^{-2}) from a solar simulator with a 150 W Xe lamp (PEC-L11, Peccell Technologies). The light intensity was calibrated with a standard silicon solar cell (BS520, Bunkoh-Keiki). The active area of each device was defined by using a 0.12 cm^2 metal mask.

Space charge limited current measurements: The current-voltage characteristics of hole only devices (ITO/PEDOT:PSS/polymer/MoO_3/Ag) were recorded with a source meter (2400, Keithley). Holes were injected from the MoO_3/Ag electrode. The device area was 1 mm^2.

External quantum efficiency measurements: The external quantum efficiency of each device was measured with monochromatic light (SM-250F, Bunkoh-Keiki). The light intensity was calibrated with a standard Si and InGaAs photodetector.

Light intensity dependence of *J-V* characteristics: The organic photovoltaic device was put in a stainless-steel chamber filled with dry N_2 (Kitano Seiki). The light source was a 5 W warm white light-emitting diode (LED; XP-G2, CREE) with a homemade condensing lens system. The LED output power was controlled so that the irradiated devices exhibited nearly identical performance to that under AM1.5, 100 mW cm^{-2} irradiation. Light intensity was altered by a combination of two neutral-density filters. The intensity was calibrated using a standard silicon photodiode (S1337-1010BQ, Bunkoh-Keiki).

Transient photocurrent measurements: The transient photocurrent measurements were performed with the same setup as for the light intensity dependence measurement. The light perturbation was performed with an N_2-dye pulsed laser (KEC-160, Usho) with

an excitation wavelength of 532 nm, a repetition rate of 10 Hz, and a pulse duration of 0.4 ns. For the transient photocurrent measurements, 20 Ω resistance was connected parallel to the input of a digital oscilloscope (DS-5632, Iwatsu), and the transient current was calculated using Ohm's law. The integral of the transient current over time provided the amount of the transient charges.

All calculations were carried out using the Gaussian 16 program.[S6] The structures were optimized with no symmetry restriction. The calculations were performed by the density functional theory method with the restricted B3LYP (Becke's three-parameter hybrid exchange functionals and the Lee-Yang-Parr correlation functional)[S7] level, using basis set 6-31G(d). Alkyl chains were replaced by methyl groups to simplify the structures and reduce the calculation costs.

Variable-angle spectroscopic ellipsometry measurement: Ellipsometry measurements were conducted with an ellipsometer (RC2, J.A. Woollam). Thin films of the organic materials were prepared on a quartz substrate. The reflected spectra with angles from 45° to 75°, the transmittance with the film normal incidence, and the transmitted spectra with angles from 0° to 50° were measured and used for analysis with the biaxial anisotropic model.

NMR spectra

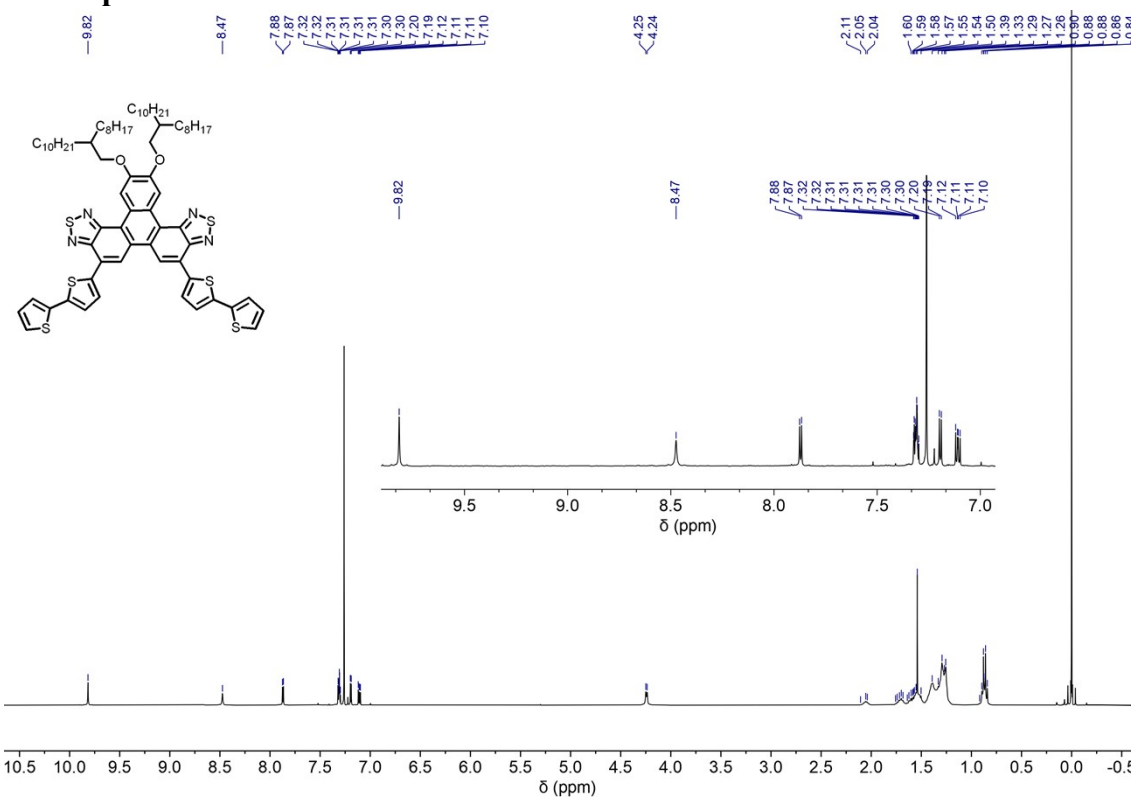

Figure S8-1. ^{1}H NMR spectrum of TPTz-2Th in $CDCl_3$ at room temperature.

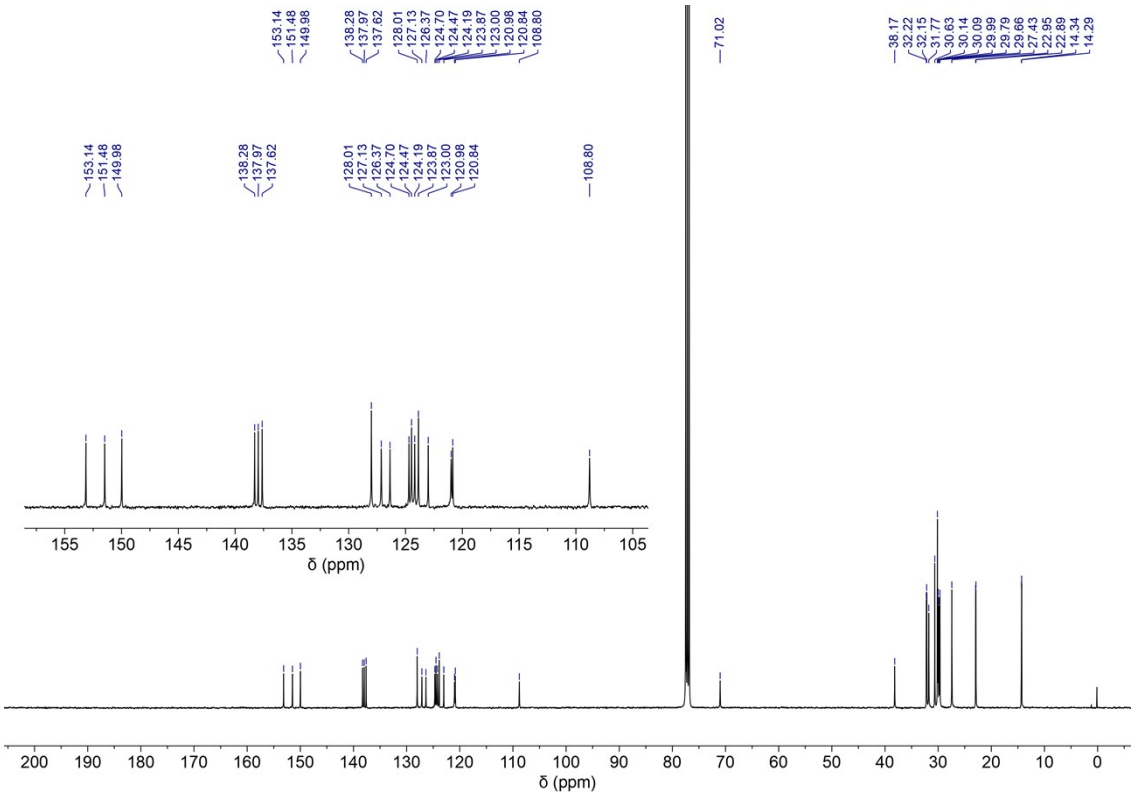

Figure S8-2. ^{13}C NMR spectrum of TPTz-2Th in $CDCl_3$ at room temperature.

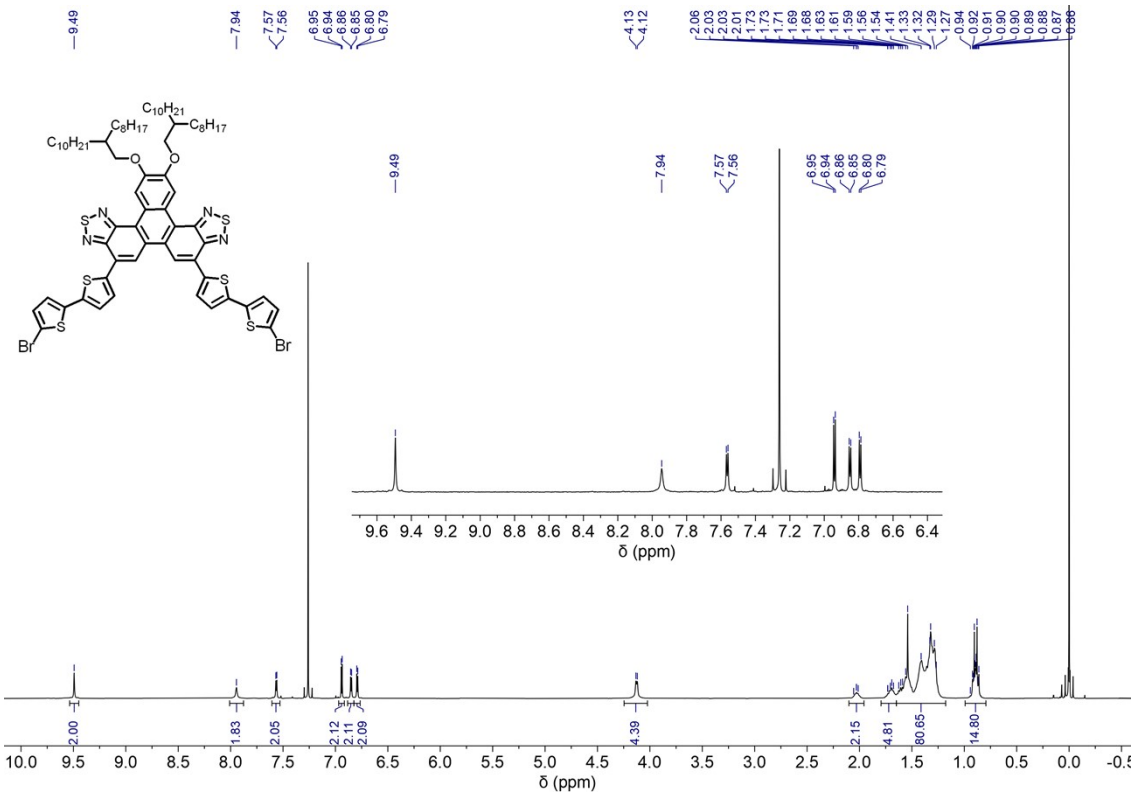

Figure S8-3. ^{1}H NMR spectrum of TPTz-2Th-Br in $CDCl_3$ at room temperature.

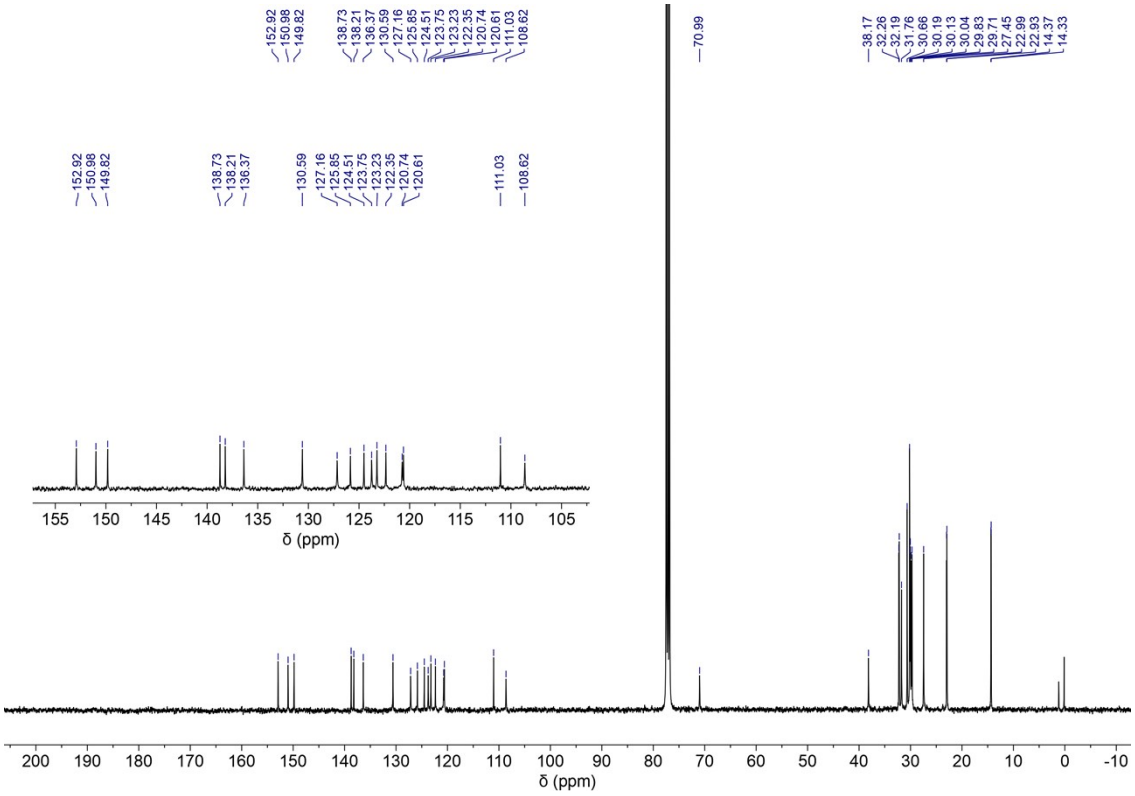

Figure S8-4. ^{13}C NMR spectrum of TPTz-2Th-Br in $CDCl_3$ at room temperature.

Mass Spectra

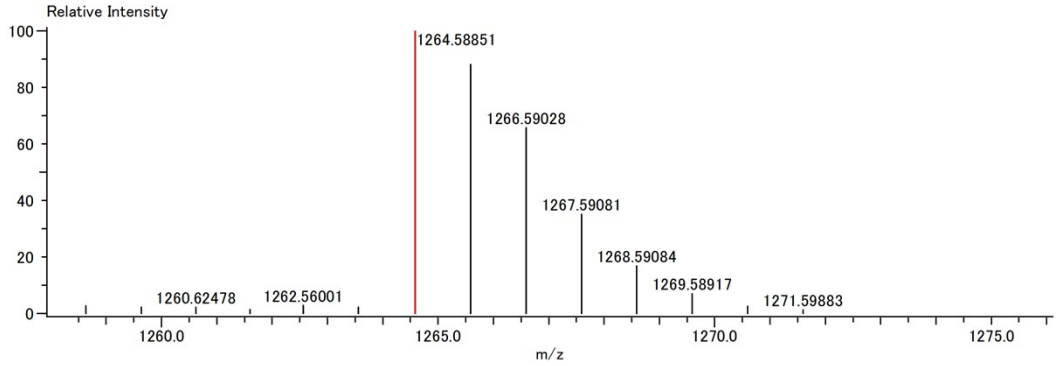

Mass	Intensity	Calc. Mass	Mass Difference [mDa]	Mass Difference [ppm]	Possible Formula	Unsaturation Number
1264.58851	82111.86	1264.58575	2.76	2.18	$^{12}C_{74}{}^{1}H_{96}{}^{14}N_{4}{}^{16}O_{2}{}^{32}S_{6}$	35.0

Figure S9-1. HRMS of TPTz-2Th.

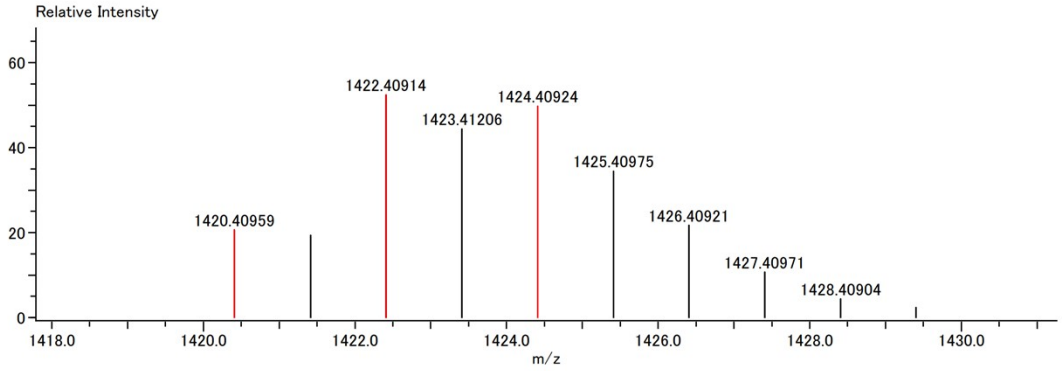

Mass	Intensity	Calc. Mass	Mass Difference [mDa]	Mass Difference [ppm]	Possible Formula	Unsaturation Number
1420.40959	17449.63	1420.40678	2.81	1.98	$^{12}C_{74}{}^{1}H_{94}{}^{79}Br_{2}{}^{14}N_{4}{}^{16}O_{2}{}^{32}S_{6}$	35.0
1422.40914	44401.28	1422.40473	4.41	3.10	$^{12}C_{74}{}^{1}H_{94}{}^{79}Br_{1}{}^{81}Br_{1}{}^{14}N_{4}{}^{16}O_{2}{}^{32}S_{6}$	35.0
1424.40924	42124.23	1424.40268	6.55	4.60	$^{12}C_{74}{}^{1}H_{94}{}^{81}Br_{2}{}^{14}N_{4}{}^{16}O_{2}{}^{32}S_{6}$	35.0

Figure S9-2. HRMS of TPTz-2Th-Br.

Supporting References

[S1] Chen, F.; Nakano, K.; Kaji, Y.; Adachi, K.; Hashizume, D.; Tajima, K. Triphenyleno[1,2-c:7,8-c']bis([1,2,5]thiadiazole) as a V-Shaped Electron-Deficient Unit to Construct Wide-Bandgap Amorphous Polymers for Efficient Organic Solar Cells, *ACS Appl. Mater. Interfaces*, **2021**, *13*, 57743.

[S2] Nakano, K.; Kaji, Y.; Tajima, K. Highly Sensitive Evaluation of Density of States in Molecular Semiconductors by Photoelectron Yield Spectroscopy in Air, *ACS Appl. Mater. Interfaces* **2021**, *13*, 28574.

[S3] Ito, Y.; Virkar, A. A.; Mannsfeld, S.; Oh, J. H.; Toney, M.; Locklin, J.; Bao, Z. Crystalline Ultrasmooth Self-Assembled Monolayers of Alkylsilanes for Organic Field-Effect Transistors, *J. Am. Chem. Soc.* **2009**, *131*, 9396.

[S4] Wei, Q.; Miyanishi, S; Tajima, K.; Hashimoto, K. Enhanced Charge Transport in Polymer Thin-Film Transistors Prepared by Contact Film Transfer Method, *ACS Appl. Mater. Interfaces.* **2009**, *1*, 2660.

[S5] Heo, S. W.; Le, T. H. H.; Tanaka, T.; Osaka, I.; Takimiya, K.; Tajima, K. Cumulative Gain in Organic Solar Cells by Using Multiple Optical Nanopatterns, *J. Mater. Chem. A* **2017**, *5*, 10347.

[S6] Gaussian 16, Revision C.01, Frisch, M. J.; Trucks, G. W.; Schlegel, H. B.; Scuseria, G. E.; Robb, M. A.; Cheeseman, J. R.; Scalmani, G.; Barone, V.; Petersson, G. A.; Nakatsuji, H.; Li, X.; Caricato, M.; Marenich, A. V.; Bloino, J.; Janesko, B. G.; Gomperts, R.; Mennucci, B.; Hratchian, H. P.; Ortiz, J. V.; Izmaylov, A. F.; Sonnenberg, J. L.; Williams-Young, D.; Ding, F.; Lipparini, F.; Egidi, F.; Goings, J.; Peng, B.; Petrone, A.; Henderson, T.; Ranasinghe, D.; Zakrzewski, V. G.; Gao, J.; Rega, N.; Zheng, G.; Liang, W.; Hada, M.; Ehara, M.; Toyota, K.; Fukuda, R.; Hasegawa, J.; Ishida, M.; Nakajima, T.; Honda, Y.; Kitao, O.; Nakai, H.; Vreven, T.; Throssell, K.; Montgomery, J. A., Jr.; Peralta, J. E.; Ogliaro, F.; Bearpark, M. J.; Heyd, J. J.; Brothers, E. N.; Kudin, K. N.; Staroverov, V. N.; Keith, T. A.; Kobayashi, R.; Normand, J.; Raghavachari, K.; Rendell, A. P.; Burant, J. C.; Iyengar, S. S.; Tomasi, J.; Cossi, M.; Millam, J. M.; Klene, M.; Adamo, C.; Cammi, R.; Ochterski, J. W.; Martin, R. L.; Morokuma, K.; Farkas, O.; Foresman, J. B.; Fox, D. J. Gaussian, Inc., Wallingford CT, **2016**.

[S7] a) A. D. Becke, A New Mixing of Hartree-Fock and Local Density-functional Theories, *J. Chem. Phys.* **1993**, *98*, 1372; b) C. Lee, W. Yang, R. G. Parr, Development of the Colle-Salvetti Correlation-energy Formula into a Functional of the Electron Density, *Phys. Rev. B* **1998**, *37*, 785.